Effect of Configuration of Diastereomers on the Electro-Optical Responses of the Antiferroelectric Phase

S.-L. Wu* and W.-J. Hsieh

Department of Chemical Engineering, Tatung University, 40 Chungshan N. Road, third Sec., Taipei, 104, Taiwan, ROC

Received May 1, 2003. Revised Manuscript Received September 2, 2003

Two diastereomers, (R)-2-butyl (S)-2-{6-[4-(4′-decyloxyphenyl)benzoyloxy]- 2-naphthyl}-propionate, (R,S)-BDPBNP, and (S)-2-butyl (S)-2-{6-[4-(4′-decyloxyphenyl)benzoyloxy]-2-naphthyl}propionate, (S,S)-BDPBNP, were prepared for investigating the effect of the configuration on mesomorphic and physical properties of the molecules. Both isomers displayed the same mesophase sequence viz. BP_{II}-N*-TGB_A*-SmA*-SmC_{AF}*, and nearly the same magnitude of spontaneous polarization at any temperature below Curie point. However, the electrooptical responses of the isomers in the SmC_{AF}* phase measured in 5-μm homogeneous cells coated with polyimide, showed that the (R,S)-isomer displayed a tristable switching, whereas the (S,S)-isomer displayed a V-shaped switching. These results suggested that V-shaped switching in antiferroelectric phase in the 5-μm cell bears no relation to the electrostatic effect of the bulk polarization but depends strongly on the absolute configuration of the diastereomers. The electrooptical responses for both isomers measured in 2-μm cells showed W-shaped switching, demonstrating the important role of the surface interaction to the switching. Further investigation in the electrooptical responses of the isomers in a 7.5-μm cell showed a significant DC threshold, double hysteresis switching, revealing that the nature of the (S,S)-isomer in the bulk possesses alternating feature of the antiferroelectricity.

Introduction

Antiferroelectric (SmC_{AF}* and SmC_A*) phases in the chiral liquid crystals exhibiting the DC threshold, double hysteresis, and tristable switching properties[1−3] were demonstrated to have the potential for fast-switching display-device applications. Thus, many compounds were synthesized and investigated to a great extent. Consequently, a correlation of the molecular structure of the materials to the appearance of the antiferroelectric liquid crystals has been successfully reviewed.[4]

Further, a mixture of antiferroelectric liquid crystals exhibiting the thresholdless, hysteresis-free, and V-shaped switching properties was found by Inui et al.[5] This switching model exhibits very attractive characteristics for the display application. Subsequently, two mixtures (Inui and Mitsui mixtures), showing V-shaped switching property have been extensively studied and reported.[5−19] And some models, such as the random model,[5,6] collective model,[13] and electrostatic model,[15,16] based on the studies of the two mixtures have been proposed to account for the nature and dynamics of the V-shaped switching. The components in these two mixtures are generally derived from a homologous series of chiral tail groups with a highly polar trifluoromethyl substituent attached to the chiral center. Consequently, the mixtures possessed high polarization; i.e., the maximum Ps value for the Inui mixture is about 170 nC/cm^2. [15]

* To whom correspondence should be addressed: E-mail: slwu@ttu.edu.tw.

(1) Chandani, A. D. L.; Hagiwara, T.; Susuki, Y.; Ouchi, Y.; Takezoe, H.; Fukuda, A. *Jpn. J. Appl. Phys.* **1988**, *27*, L729.
(2) Chandani, A. D. L.; Ouchi, Y.; Takezoe, H.; Fukuda, A.; Terahima, K.; Furukawa, K.; Kishi, A. *Jpn. J. Appl. Phys.* **1989**, *28*, L1261.
(3) Fukuda, A.; Takanishi, Y.; Iasozki, T.; Ishikawa, K.; Takezoe, H. *J. Mater. Chem.* **1994**, *4*, 997.
(4) Goodby, J. W.; Slany, A. J.; Booth, C. J.; Nishyama, I.; Vuijk, J. D.; Syring, P.; Toyne, K. J. *Mol. Cryst. Liq. Cryst.* **1994**, *243*, 231.
(5) Inui, S.; Limura, N.; Suruki, T.; Iwane, H.; Miyachi, F.; Takanoshi, Y.; Fukuda, A. *J. Mater. Chem.* **1996**, *6*, 671.
(6) Seomun, S. S.; Takanishi, Y.; Ishikawa, K.; Takezoe, H.; Fukuda, A. *Jpn. J. Appl. Phys.* **1997**, *36*, 3586.
(7) Fukuda, A.; Seomun, S. S.; Takanashi, T.; Takanishi, Y.; Ishikawa, K. *Mol. Cryst. Liq. Cryst.* **1997**, *303*, 379.
(8) Seomun, S. S.; Takanashi, Y.; Ishikawa, K.; Takezoe, H.; Fukuda, A.; Tanaka, C.; Fujiama, T.; Maruyama, T.; Nishiyama, S. *Mol. Cryst. Liq. Cryst.* **1997**, *303*, 181.
(9) Seomun, S. S.; Park, B.; Chandani, A. D. L.; Hermann, D. S. *Jpn. J. Appl. Phys.* **1998**, *37*, L691.
(10) Matsumoto, T.; Fukuda, A.; Johno, M.; Motoyama, Y.; Yui, T.; Seomun, S. S.; Yamashita, M. *J. Mater. Chem.* **1999**, *9*, 2051.
(11) Seomun, S. S.; Gouda, T.; Takanishi, Y.; Ishikawa, K.; Takezoe, H. *Liq. Cryst.* **1999**, *26*, 151.
(12) Chandani, A. D. L.; Cui, Y.; Seomun, S. S.; Takanishi, Y.; Ishikawa, K.; Takezoe, H.; Fukuda, A. *Liq. Cryst.* **1999**, *26*, 167.
(13) Park, B.; Seomun, S. S.; Nakata, M.; Takahashi, M.; Takanishi, Y.; Ishikawa, K.; Takezoe, H. *Jpn. J. Appl. Phys.* **1999**, *38*, 1474.
(14) Fukuda, A.; Matsumoto, T. *Mol. Cryst. Liq. Cryst.* **1999**, *328*, 1.
(15) Rudquist, R.; Lagerwall, J. P. F.; Buivydas, M.; Gouda, F.; Lagerwall, S. T.; Clark, N. A.; Maclennan, J. E.; Shoa, R.; Coleman, D. A.; Bardon, S.; Bellini, T.; Link, D. R.; Natale, G.; Glaser, N. A.; Walba, D. M.; Wand, M. D.; Chen, X.-H. *J. Mater. Chem.* **1999**, *9*, 1257.
(16) Clark, N. A.; Coleman, D.; Maclennan, J. E. *Liq. Cryst.* **2000**, *27*, 985.
(17) Takechi, M.; Chao, K.; Ando, T.; Matsumoto, T.; Fukuda, A.; Yamashita, M. *Ferroelectrics* **2000**, *246*, 1.
(18) Shibahara, S.; Yamamoto, J.; Takanishi, Y.; Ishikawa, K.; Takezoe, H. *Jpn. J. Appl. Phys.* **2001**, *40*, 5026.
(19) Hayashi, N.; Kato, T.; Aoki, T.; Ando, T.; Fukuda, A.; Seomun, S. S. *Phys. Rev. Lett.* **2001**, *87*, 15701.

10.1021/cm0303843 CCC: $25.00
Published on Web 10/11/2003

Scheme 1. Synthetic Procedures for the Diasteromeric Materials (R,S)- and (S,S)-BDPBNP

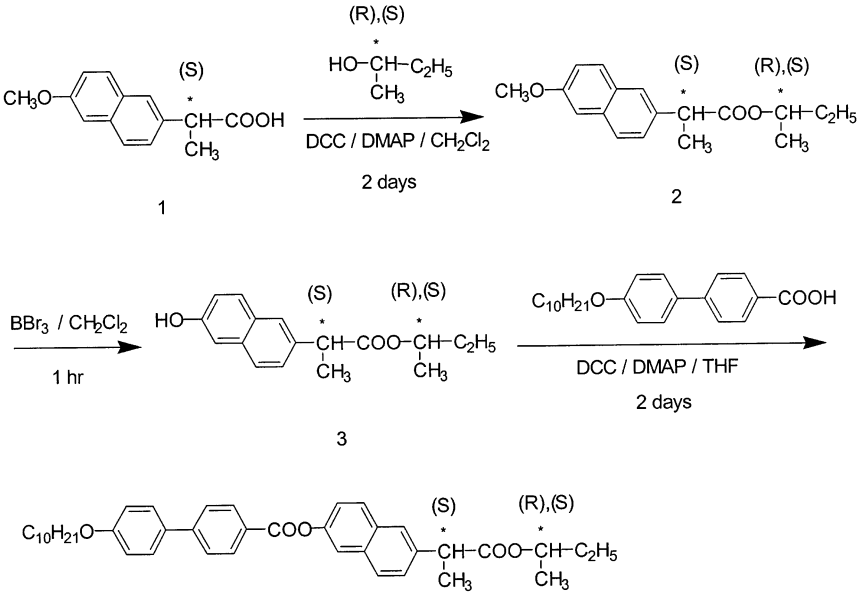

The electrooptical response that resulted in a V-shaped switching property has been realized to critically depend on the temperature, frequency, and the polarity of the alignment surface. A few studies, however, have reported the effect of molecular structure of the liquid crystals on the switching behavior.[12] Recently, we reported a homologous series of chiral swallow-tailed materials, 1-ethylpropyl (S)-2-{6-[4-(4′-alkyloxyphenyl)-benzoyloxy]-2-naphthyl}propionate, (S)EP*m*PBNP, showing antiferroelectric liquid crystal phase with the thresholdless, V-shaped switching property.[20,21] The antiferroelectric phase of this material was found to possess relatively low polarization (maximum Ps = 30 nC/cm^2) as compared to that reported from the Inui and Mitsui mixtures. This phenomenon suggests that V-shaped switching could be obtained in the materials with low polarization in antiferroelectric phase.

In this paper we report, from the molecular structure point of view, two diastereoisomers showing different electrooptical responses in the antiferroelectric phase. These two diastereomers are (R)-2-butyl (S)-2-{6-[4-(4′-decyloxyphenyl)benzoyloxy]-2-naphthyl}propionate, (R,S)-BDPBNP, and (S)-2-butyl (S)-2-{6-[4-(4′-decyloxyphenyl)-benzoyloxy]-2-naphthyl}propionate, (S,S)-BDPBNP, and have the general structural formula shown below.

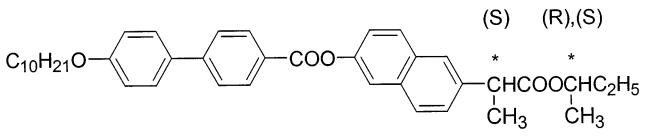

Experimental Section

Characterization of Materials. The chemical structures of intermediates and target materials were analyzed by nuclear magnetic resonance spectroscopy using a JEOL EX-400 FT-NMR spectrometer. The purity of the materials was checked by thin-layer chromatography and further confirmed by elemental analysis using a Perkin-Elmer 2400 spectrometer. The specific rotations of the chiral materials were measured in dichloromethane using a JASCO DIP-360 digital polarimeter.

Mesophases were principally identified by microscopic texture of the materials sandwiched between two glass plates under crossed polarizing microscope using a Nikon Microphot-FXA in conjunction with a Mettler FP82-HT or Instec HS1 hot stages. Transition temperatures and phase transition enthalpies of the materials were determined by differential scanning calorimetry using a Perkin-Elmer DSC7 calorimeter at running rates from 1 to 20 °C/min. The antiferroelectric phase of the materials was further characterized by switching behavior electrooptical response in homogeneously aligned cells coated with polyimide film, which were purchased from E. H. C. Co., Japan. The sample was filled into the liquid crystal sample cell by capillary action in the isotropic state. Two wires were then pasted separately to the ITO glasses of the sample cell by silver paint.

The response of optical transmittance versus applied electric field was recorded using a He−Ne laser (5 mW, 632.8 nm) as a probe beam.[22,23] The optical transmittance of the probe beam that passed through the cells between the crossed polarizers (whose axes were parallel and perpendicular, respectively, to the smectic layer normal) was detected by a photodiode. The signals were monitored by digital oscilloscope (HP54502A). The voltage applied to the cell was produced by an arbitrary waveform generator (AG1200) and amplified by a homemade power preamplifier.

The magnitude of spontaneous polarization (Ps) was measured by a triangular wave method.[24] A triangular waveform was applied to the sample from a YOGAW AG1200 arbitrary waveform generator. The induced current was displayed by measuring the voltage across a wire-wound resistor using a Hewlett-Packard HP54502A digital storage oscilloscope.

Preparation of Materials. The starting chiral material for the synthesis was (S)-2-(6-methoxy-2-naphthly)propionic acid, purchased from Tokyo Chemical Industry (TCI) Co. Ltd., Japan, with optical purity greater than 99% enantiomeric excess. Tetrahydrofuran (THF) and dichloromethane (CH_2Cl_2), were dried by treating with $LiAlH_4$ and CaH_2, respectively, and distilled before use. The synthetic procedures were carried out in a manner similar to that described previously[25] and are shown in Scheme 1. The acid **1** was esterified with (R)-2-butanol in the presence of *N*,*N*-dicyclohexylcarbodiimide (DCC)

(20) Wu, S.-L.; Hsieh, W.-J. *Chem. Mater.* **1999**, *11*, 852.
(21) Wu, S.-L.; Chang, P.-L. *Liq. Cryst.* **2002**, *29*, 1355.
(22) Chandani, A. D. L.; Hagiwara, T.; Suzuki, Y.; Ouchi, Y.; Takezoe, H.; Fukuda, A. *Jpn. J. Appl. Phys.* **1988**, *27*, L729.
(23) Lee, J.; Chandani, A. D. L.; Itoh, K.; Ouchi, Y.; Takezoe, H.; Fukuda, A. *Jpn. J. Appl. Phys.* **1990**, *29*, 1122.
(24) Miyasato, K.; Abe, S.; Takazoe, H.; Fukuda, A.; Kuze, T. *Jpn. J. Appl. Phys.* **1983**, *22*, L661.
(25) Wu, S.-L.; Yen, P. C.; Hsieh, W.-J. *Liq. Cryst.* **1998**, *24*, 741.

Table 1. Transition Temperature and Enthalpies Δ*H* (in italics) of Diastereomeric Materials (R,S)- and (S,S)-BDPBNP at 2 °C min^{-1} Scanning Rate

absolute configuration	T/°C and ΔH/ Jg^{-1} (in italics)						
	Iso−BP_{II}	BP_{II}−N*	N*−TGB_A*	TGB_A*−SmA*	SmA*−SmC_{AF}*	SmC_{AF}*−Cr.	mp[b]
R,S	141.9	139.4	135.6	131.9	112.9	71.8	97.0
	4.0	a	a	a	0.4	34.2	39.0
S,S	141.8	139.3	135.7	133.4	109.8	69.7	93.5
	4.3	[a]	[a]	[a]	*0.3*	*35.8*	*42.3*

[a] The enthalpies of the TGB_A−SmA*, N*−TGB_A, and BP_{II}−N* transitions were added to the Iso−BP_{II} transition value. [b] mp refers to melting point taken from DSC thermograms recorded at heating rates of 2 °C min^{-1}.

and 4-(dimethylamino)pyridine (DMAP) to produce the ester, (R)-2-butyl (S)-2-(6-methoxy-2-naphthyl)propionate **2**. The methoxy group of the ester was demethylated by treatment with BBr_3, and the resulting hydroxy group of (R)-butyl (S)-2-(6-hydroxy-2-naphthyl)propionate, **3**, was subsequently esterified with 4-(4′-decyloxyphenyl)benzoic acid **4**, using DCC and DMAP to produce the target compound, (R)-2-butyl (S)-2-{6-[4-(4′-decyloxyphenyl)benzyloxy]-2-naphthy}propionate, (R,S)-BDPBNP. The diasteromeric isomer, (S,S)-BDPBNP, was prepared in the same manner by using (S)-2-butanol as the second chiral starting material. All the intermediates and final products were purified by column chromatography passing over silica gel and using dichloromethane as eluent. The analytical data for the synthetic intermediates and target materials are provided below.

(R)-2-Butyl (S)-2-(6-methoxyl-2-naphthyl)propionate. Yield: 82%. Elemental analysis for $C_{18}H_{22}O_3$ (%): calculated, C 75.50, H 7.74; found, C 75.47, H 7.78. ^{1}H NMR ($CDCl_3$): δ (ppm) 0.7−1.7 (m, 11H, RCH_2CH_3), 3.88 (q, 3H, OCH_3), 3.79−3.85 (q, 1H, ArCHCOO), 4.8−4.9 (m, 1H, COOCH), 7.1−7.7 (m, 6H, ArH).

(S)-2-Butyl (S)-2-(6-methoxy-2-naphthyl)propionate. Yield: 90%. Elemental analysis for $C_{18}H_{22}O_3$ (%): calculated, C 75.50, H 7.74; found, C 75.49, H 7.76. ^{1}H NMR ($CDCl_3$): δ (ppm) 0.8−1.3 (m, 13H, RCH_2CH_2), 3.9 (q, 3H, OCH_3), 3.8−3.9 (q, 1H, ArCHCOO), 4.8−4.9 (m, 1H, COOCH), 7.1−7.7 (m, 6H, ArH).

(R)-2-Butyl (S)-2-(6-hydroxy-2-naphthyl)propionate. Yield: 64%. Elemental analysis for $C_{17}H_{20}O_3$ (%): calculated, C 74.97, H 7.40; found, C 74.94, H 7.45. ^{1}H NMR ($CDCl_3$): δ (ppm) 1.1−1.8 (m, 11H, RCH_2CH_3), 3.8−3.9 (q, 1H, ArCHCOO), 4.8−4.9 (m, 1H, COOCH), 5.7 (s, 1H, OH), 7.0−7.7 (m, 6H, ArH). Specific rotation $[\alpha]_D^{26}$ = +46.92° (c: 0.645 g/100 mL, CH_2Cl_2).

(S)-2-Buthyl (S)-2-(6-hydroxy-2-naphthyl)propionate. Yield: 81%. Elemental analysis for $C_{17}H_{20}O_3$ (%): calculated, C 74.97, H 7.40; found, C 74.90, H 7.37. ^{1}H NMR ($CDCl_3$): δ (ppm) 0.8−1.3 (m, 11H, RCH_2CH_3), 3.8−3.9 (q, 1H, ArCHCOO), 4.8−4.9 (m, 1H, COOCH), 5.9 (s, 1H, OH), 7.1−7.7 (m, 6H, ArH). Specific rotation $[\alpha]_D^{26}$ = +46.92° (c: 0.645 g/100 mL, CH_2Cl_2).

(R)-2-Butyl (S)-2-{6-[4-(4′-decyloxyphenyl)benzoyloxy]-2-naphthyl}propionate, (R,S)-BDPBNP. Yield: 84%. Elemental analysis for $C_{34}H_{48}O_5$ (%): calculated, C 78.91, H 7.95; found, C 78.98, H 8.00. ^{1}H NMR ($CDCl_3$): δ (ppm) 0.7−1.9 (m, 40H, RCH_2CH_3), 3.8−3.9 (q, 1H, ArCHCOO), 4.0−4.1 (t, 2H, OCH2), 4.6−4.8 (m, 1H, COOCH), 7.0−8.3 (m, 14H, ArH). Specific rotation $[\alpha]_D^{26}$ = +18.86° (c: 0.645 g/100 mL, CH_2Cl_2).

(S)-2-Butyl (S)-2-{6-[4-(4′-decyloxyphenyl)benzoyloxy]-2-naphthyl}propionate, (S,S)-BDPBNP. Yield: 84%. Elemental analysis for $C_{34}H_{48}O_5$ (%): calculated, C 78.90, H 7.95; found, C 78.94, H 7.98. ^{1}H NMR ($CDCl_3$): δ (ppm) 0.8−1.3 (m, 30H, RCH_2CH_3), 3.9 (q, 1H, ArCHCOO), 4.1 (t, 2H, OCH_2), 4.8−4.9 (m, 1H, COOCH), 7.0−8.3(m, 14H, ArH). Specific rotation $[\alpha]_D^{26}$ = +18.87 (c: 0.659 g/100 mL, CH_2Cl_2).

Results and Discussion

Mesomorphic Properties. The mesophases and their corresponding phase transition temperatures for (R,S)- and (S,S)-isomers are given in Table 1. Both materials exhibit enantiotropic BP_{II}, N*, TGB_A*, SmA*, and antiferroelectric SmC_{AF}* phases. The BP_{II} was characterized by forming some blue-gray platelets. The N* phase was obtained with small focal-conic and/or Grandjean planar texture. The TGB_A* phase was recognized by the appearance of filaments. This phase has been found in many compounds such as those containing phenylpropiolate,[26−30] tolane core,[31−35] and naphthyl unit,[20,36−39] in which the core structure is the same as both diastereomers, and so on. The filaments emerged and formed paramorphotic texture of the SmA* phase. The SmC_{AF}* phase was primarily characterized by the appearance of striated focal-conic and pseudo-homeotropic texture.

To further identify the SmC_{AF}* phase for the isomers, materials were filled into 2-μm thickness of homogeneously aligned cells. Because of the existence of the TGB_A* phase, the quality of alignment in the SmA* phase was rather poor. However, it was improved by applying an electrical field at the SmC_{AF}* phase for several hours and then heated to the SmA* phase. After the treatment, the texture of the SmA* phase was altered from the birefringence texture to the normal SmA* texture. A needlelike defect perpendicular to the smectic layer normal accompanying the fringe lines parallel to the smectic layer normal was noticed while the phase transition from SmA* to SmC_{AF}* occurred. Rotation of the sample showed that the bright and dark stripes alternated with each other. In addition, the average extinction direction was aligned along the direction perpendicular to the molecular layers. The above phenomena support the assignment of antiferroelectric SmC_{AF}* phase as reported by Nishiyama et al.[40] However, after the application of an electric field (100

(26) Goodby, J. W.; Waugh, M. a.; Stein, S. M.; Chin, E.; Pindak, R.; Patel, J. S. *Nature* **1989**, *337*, 449.
(27) Goodby, J. W.; Waugh, M. a.; Stein, S. M.; Chin, E.; Pindak, R.; Patel, J. S. *J. Am. Chem. Soc.* **1989**, *111*, 8119.
(28) Goodby, J. W.; Nishiyama, I.; Slaney, A. J.; Booth, C. J.; Toyne, K. J. *Liq. Cryst.* **1993**, *14*, 37.
(29) Booth, C. J.; Goodby, J. W.; Toyne,; K. J.; Dummur, D. J.; Kang, J. S. *Mol. Cryst. Liq. Cryst.* **1997**, *260*, 39.
(30) Goodby, J. W. *Mol. Cryst. Liq. Cryst.* **1995**, *292*, 245.
(31) Nguyen, H. T.; Bouchta, A.; Navailles, L.; Barois, P.; Isaert, N.; Twjeg, R. J.; Marroufi, A.; Destrade, C. *J. Phys. France II* **1992**, *2*, 1889.
(32) Bouchta, A.; Nguyen, H. T.; Navailles, L.; Barois, P.; Destrade, C.; Bougrioua, F.; Isaert, N. *J. Mater. Chem.* **1995**, *5*, 2079.
(33) Navailles, L.; Nguyen, H. T.; Barois, P.; Isaert, N.; Delord, P. *Liq. Cryst.* **1996**, *20*, 653.
(34) Li, M.-H.; Nguyen, H. T.; Sigaud, G.; Barois, P.; Isaert, N.; Delord, P. *Liq. Cryst.* **1997**, *23*, 389.
(35) Shao, R.; Pang, J.; Clark, N. A.; Rego, J. A.; Walba, D. M. *Ferroelectrics* **1993**, *147*, 255.
(36) Hsiue, G.-H.; Hwang, C.-P.; Chen, J. H.; Chang, R.-C. *Liq. Cryst.* **1996**, *20*, 45.
(37) Wu, S.-L.; Hsieh, W.-J. *Liq. Cryst.* **1996**, *21*, 783.
(38) Hsieh, W.-J.; Wu, S.-L. *Mol. Cryst. Liq. Cryst.* **1997**, *302*, 253.
(39) Wu, S.-L.; Yen, P. C.; Hsieh, W.-J. *Liq. Cryst.* **1998**, *24*, 741.
(40) Nishiyama, I.; Goodby, J. W. *J. Mater. Chem.* **1992**, *2*, 1015.

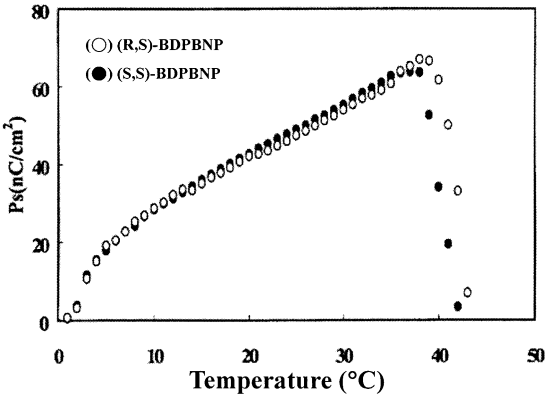

Figure 1. Magnitudes of the spontaneous polarization plotted as a function of temperature for the diastereomers (R,S)-BDPBNP and (S,S)-BDPBNP: (○) (R,S)-isomer, and (■) (S,S)-isomer.

Hz, 20 V_{PP}), the texture was changed in such a way that the stripes gradually disappeared and were followed by the appearance of dechiralization lines perpendicular to the layer normal. This possibly suggests that the ferroelectric domains appeared, although antiferroelectric domains still remained. The SmC_{AF}* phase was irreversible as it was changed to the ferroelectric SmC* phase on application of an electric field, suggesting that the SmC_{AF}* phase is unstable in the thinner cell, similar to that reported by Suzuki et al.[41]

It is worth pointing out that both the (R,S)- and (S,S)-isomers displayed frustrated phases: blue phase and TGB_A* phase, and SmC_{AF}* phase in the same temperature ranges, indicating that both isomers have the same molecular chirality and have no reduction in the chirality of the system on moving from a (R,S)-configuration to a (S,S)-configuration. Thus, the formation of TGB_A* phase may not be attributed by the increasing molecular chirality exclusively, but presumably by the weakening of layer structure from the steric effect. The introduction of a methyl substituent group at the chiral tail would disturb the packing ability of the molecules; thereby reduce the tendency to form a lamellar arrangement and weakening the layer ordering.

The DSC thermograms for both isomers on heating and cooling at a scanning rate of 5 °C/min displayed nearly the same thermal traces. The SmC_{AF}*−SmA* transition showed the first-order characteristics as observed for other compounds that display antiferroelectric tendendency.[40,42] There are four endothermic peaks correspond to the SmA*−TGB_A*, TGB_A*−N*, N*−BP_{II}, and BP_{II}−Iso transitions nearing the clearing point.

Spontaneous Polarization. The magnitudes of the spontaneous polarizations (Ps) for the isomers are plotted in Figure 1. The Ps values increase rapidly in the vicinity of the SmA*−SmC_{AF}* transition and then increase gradually before crystallization. It is shown that the magnitudes of Ps obtained from both isomers are nearly the same at any temperature below the Curie

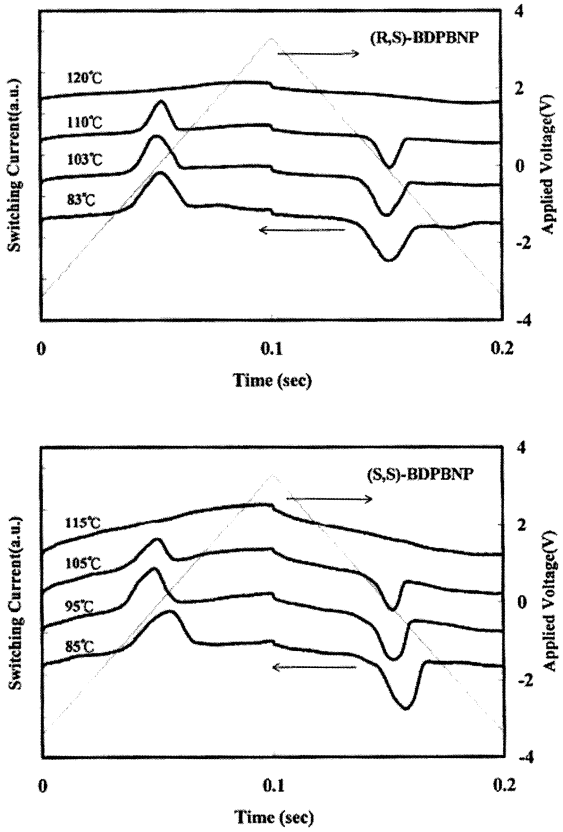

Figure 2. Switching current behaviors measured in the SmA* and SmC_{AF}* phases for (a) (R,S)-isomer and (b) (S,S)- isomer in the homogeneously aligned cell with 5-μm thickness.

point in the SmC_{AF}* phase. It is generally acknowledged that, if the dipole associated with the first chiral center is enhanced by the second chiral center, one might expect the chirality to be increased. Or it might be possible that the dipoles of two chiral centers may oppose each other and the effective molecular chirality of the system may therefore be reduced. Thus, the apparent results of polarization obtained from these two isomers strongly suggest that the addition of second chiral group and/or the absolute configuration of the diasteromeric chiral tails have no significant contribution on the overall molecular transverse dipole strength in the SmC_{AF}* phase. A conceivable explanation of the result can be presumably rationalized as that the second chiral center may not be able to trap along the long molecular axis due to the peripheral alkyl chain length attached to the second chiral center, which is too short.[43] This means that the overall molecular transverse dipole strength is not affected by the dipoles associated with each chiral center being additive or subtractive in the molecules.

Switching Behavior and Electrooptical Response. The switching current behaviors of both of the isomers in the SmC_{AF}* phase were measured in a 5-μm homogeneous cell, and the switching profiles are presented in Figure 2. Surprisingly, as it can be seen that only one broadened current peak appears in the whole temperature range of SmC_{AF}* phase for both isomers. This is different from that detected from the normal

(41) Suzuki, Y. I.; Isozaki, T.; Hashimoto, S.; Kusumoto, T.; Hiyama, T.; Takanishi, T.; Takezoe, H.; Fukuda, A. *J. Mater. Chem.* **1996**, *6*, 753.

(42) Inui, S.; Kawano, S.; Saito, M.; Iwane, H.; Takanishi, Y.; Hiraoka, K.; Ouchi, Y.; Takezoe, H.; Fukuda, A. *Jpn. J. Appl. Phys.* **1990**, *29*, 987.

(43) Goodby, J. W.; Patel, J. S.; Chin, E. *J. Phys. Chem.* **1987**, *91*, 5151.

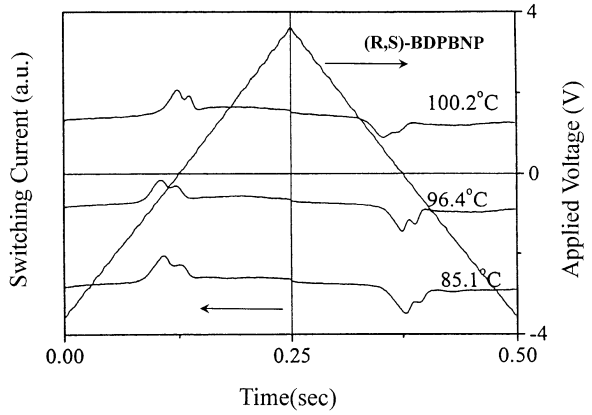

Figure 3. Switching current behaviors measured in the SmC_{AF}* phase for (R,S)-isomer in the homogeneously aligned cell with 5-μm thickness.

antiferroelectric phase such as MHPOBC,[44] but resembles that reported as the SmC* phase in an antiferroelectric mixture with thresholdless, V-shaped switching property.[6,10] However, the broad band switching peak can also be split into two overlapping peaks on the variation of frequency as shown in Figure 3. This result is similar to ours previously reported for an antiferroelectric compound with thresholdless, V-shaped switching property.[20] The antiferroelectric character of these two isomers was further identified by the measurement of the optical responses.

The electrooptical responses in the SmC_{AF}* phase for both isomers were detected by using different thicknesses of homogeneous cells to explore the real nature of the phase, and the results are presented in Figure 4. It can be seen that the electrooptical response of the (R,S)-isomer shows a switching of double hysteresis loops; a typical antiferroelectric electrooptical feature, while that of the (S,S)-isomer shows a V-shaped switching in the SmC_{AF}* phase at 5-μm cell. Theses results reveal that the electrooptical response in the antiferroelectric phase is remarkably dependent on the configuration of the molecules containing two chiral centers in the chiral tail. It is worth pointing out again that the magnitudes of polarization for both isomers are nearly the same at the same temperature below Curie point. Thus, the formation of different switching behaviors strongly suggests that the formation of V-shaped switching is not caused by the electrostatic effect of polarization in the bulk of liquid crystal molecules, rather it is caused by the different absolute/spatial configuration of the molecular structure at the chiral tails of the materials. It is then concluded that, in the fixed conditions of the cell such as homogeneously aligned layer of polyimide and cell thickness, molecular structure of the materials plays a very important role in the formation of the V-shaped switching property.

The electrooptical responses for both isomers at a 2-μm cell, however, display a W-shaped switching property as shown in Figure 4. The double hysteresis switching of (R,S)-isomer and V-shaped switching of (S,S)-isomer in a 5-μm cell are altered to the W-shaped switching in the 2-μm cell. This result implies an

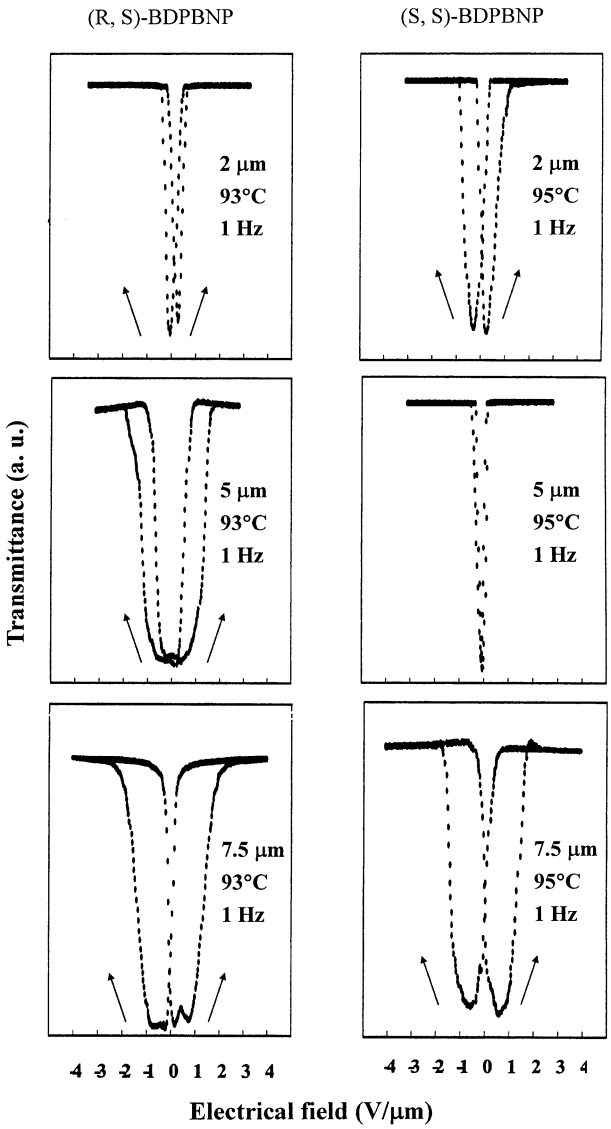

Figure 4. Optical transmittance versus electrical field measured by applying triangular waveform to the SmC_{AF}* phase of diastereomers in 2-, 5-, and 7.5-μm thickness of homogeneously aligned cells.

importance of the surface interaction force that exerted to the bulk of the liquid crystal in the cell. Thus, it can be realized that the effective forces induced by the surface interaction to give a V-shaped switching in the (S,S)-isomers in the 5-μm cell should exert its effect uniformly throughout the bulk of the liquid crystal in the antiferroelectric phase. Further investigation of the isomers in 7.5-μm cells showed that the electrooptical responses for both isomers display a double hysteresis switching property. As the cell gap increases in the cell, the force that raised from the surface interaction to the bulk of liquid crystals could expect to be reduced. Because the V-shaped switching property is considered the result of surface-induced phenomenon, the electrooptical response in a 7.5-μm cell showing double hysteresis loop should reflect to some extent the nature of the materials in the antiferroelectric phase. Studies of the free-standing film from the antiferroelectric mixture that possesses a V-shaped switching property also reported that the mixture displays alternating features of antiferroelectric structure.[8]

(44) Fukuda, A.; Takanishi, Y.; Isozaki, J.; Ishikawa, K.; Takezoe, H. *J. Mater. Chem.* **1994**, *4*, 997.

Conclusion

We have demonstrated that two diastereomers, (R,S)-BDPBNP and (S,S)BDPBNP, exhibit antiferroelectric SmC_{AF}* phase. Both isomers have the same magnitudes of spontaneous polarization at any temperature below the Curie point. The electrooptical responses of the isomers in the SmC_{AF}* phase are critically dependent on the temperatures, frequency, and thickness of the homogeneous cell. It is concluded that the V-shaped switching property in 5-μm cells does not result from the electrostatic effect of the polarization in the bulk of the liquid crystal molecules, but rather is caused by the configuration of the isomers that contain two chiral centers in the chiral tail of the materials. The nature of the molecular structure which formed the V-shaped switching property in the SmC_{AF}* phase is, as that reported from the study of free-standing film, an antiferroelectric feature of the alternating structure.[11]

CM0303843